Highly Nonlinear Fibers and Their Applications

Govind P. Agrawal

Institute of Optics
University of Rochester
Rochester, NY 14627

Introduction

- Many nonlinear effects inside optical fibers depend on the parameter $\gamma = 2\pi n_2/(\lambda A_{\text{eff}})$.

- Kerr coefficient $n_2 \approx 2.6 \times 10^{-20}$ m^2/W for silica fibers.

- For telecommunication fibers, A_{eff} is close to 80 μm^2, resulting in $\gamma \sim 1$ W^{-1}/km.

- This value is too small for most nonlinear applications of optical fibers, forcing one to employ high peak powers and long fiber lengths.

- Highly nonlinear fibers (HNLFs) solve this problem by reducing A_{eff} or/and using non-slica materials.

- The nonlinear parameter $\gamma > 10$ W^{-1}/km for HNLFs and may even exceed 1000 W^{-1}/km in some cases.

Highly Nonlinear Fibers

Four different approaches employed in practice:

- Narrow-core fibers with Silica Cladding: A narrow core and high doping levels reduce A_{eff} and enhance γ.

- Tapered Fibers with Air Cladding: Standard fibers stretched by a factor of 50 or more; surrounding air acts as the cladding.

- Microstructured Fibers: Air holes introduced within the cladding; photonic crystal fibers, holey fibers, etc.

- Non-silica Fibers: Use a different material with large values of n_2 such as lead silicates, chalcogenides, tellurite oxide, bismuth oxide.
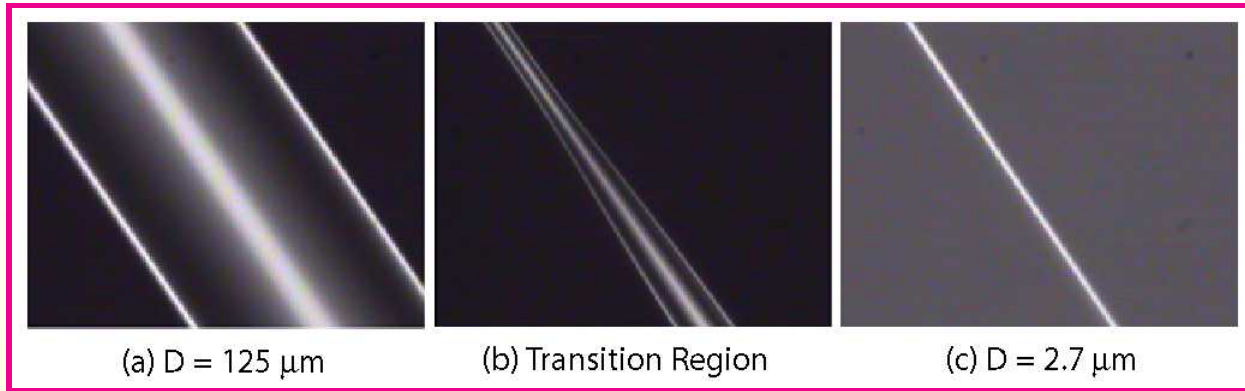
Tapered Fibers

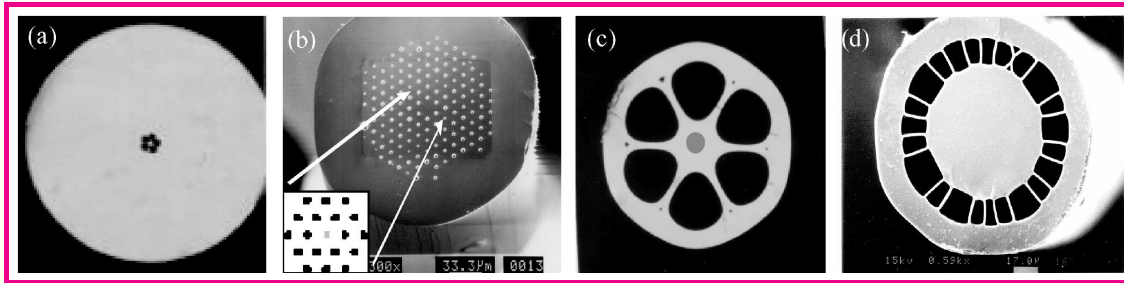(a) D = 125 μm   (b) Transition Region   (c) D = 2.7 μm

(Lu and Knox, Opt. Exp. **12**, 347, 2004)

- Fiber stretched to reduce its cladding diameter to ~2 μm.

- Air acts as the cladding material for the new narrow core.

- A large index step ($\Delta n = 0.45$) keeps the mode confined to the new core even when core diameter is 1 μm or less.

- Tapered fibers often support multiple modes ($V > 2.405$).

Microstructured Fibers

(a)   (b)   (c)   (d)

(Eggleton et al, Opt. Exp.**9**, 698, 2001)

- A narrow core is surrounded by a silica cladding with embedded air holes.

- Number of air holes varies from structure to structure.

- Hole size can vary from < 1 μm to > 5 μm depending on the fiber design.

- Such fibers are also called holey fibers or *photonic crystal fibers* (PCF) depending on design details.

Photonic Crystal Fibers

- PCFs were first made in 1996 (Russell's group); cladding contained a 2D periodic array of air holes.

- It was realized later that the periodic nature of air holes was not critical as long as the cladding has multiple air holes that reduce its refractive index below that of the silica core.

- Periodic nature becomes important in photonic bandgap fibers.

- The core of such fibers often contains air to which light is confined by the photonic bandgap.

- Such truly PCFs can act as a highly nonlinear medium if air is replaced with a suitable gas or liquid.

- When air was replaced with hydrogen, stimulated Raman scattering was observed at 100 times lower pulse energies.
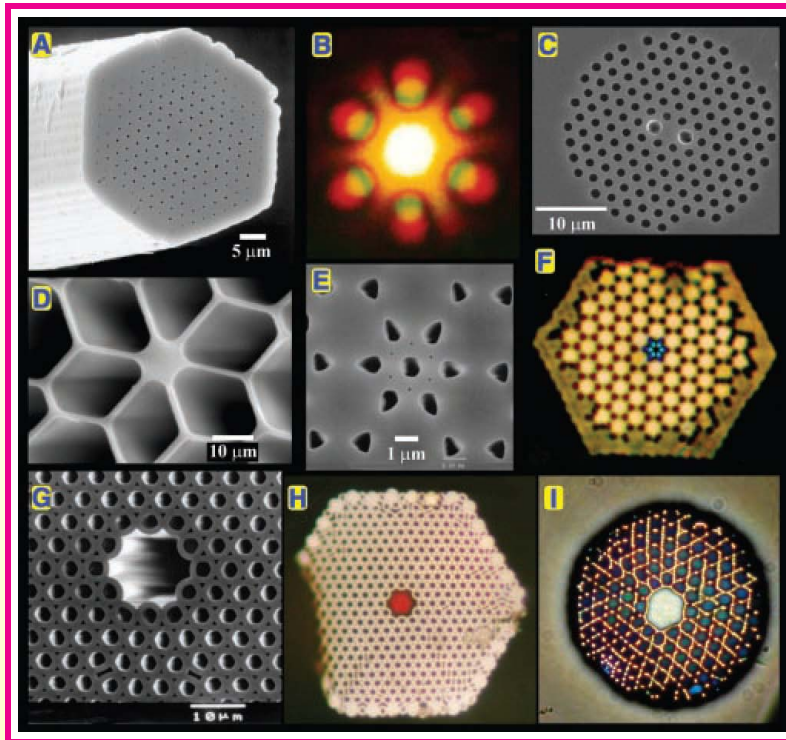
# Photonic Crystal Fibers

P. St. J. Russell, Science **299**, 358 (2003)

Fabrication Technique

- A perform is first made by stacking capillary tubes of pure silica (Ruselll, Science, **299**, 358, 2003).

- Preform is then drawn into a fiber.

- A polymer coating added to protect the fiber.

- Air channel created by removing the central rod.

- This channel can later be filled with a gas or liquid that acts as the nonlinear medium.

- Extrusion technique is also used for some holey fibers.

- Preform is made by extruding material selectively from a solid rod by forcing it through a die.
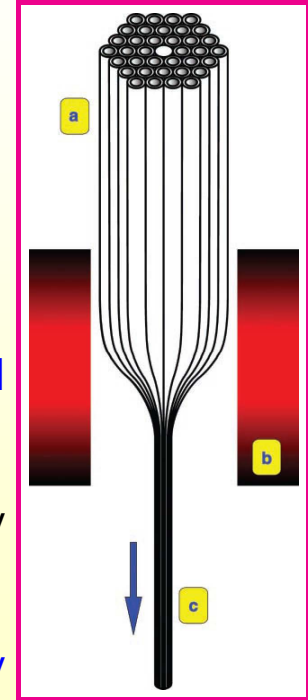
Non-silica Fibers
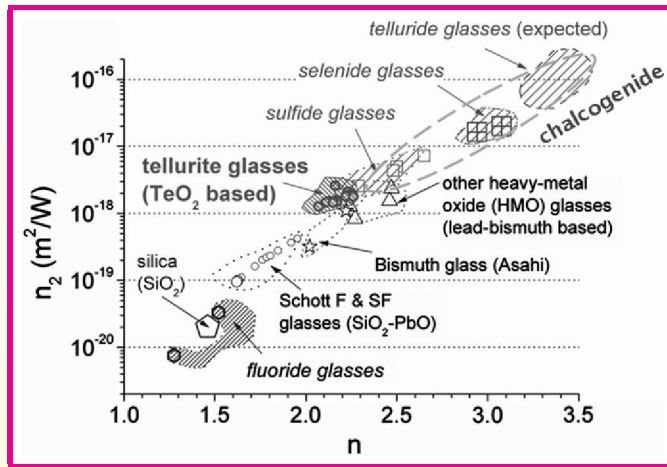
(Feng et al., Opt. Fiber Technol. **16**, 378, 2010)

- Glasses with larger nonlinearities can be used to make fibers.

- These include lead silicates (SF), chalcogenides, tellurite oxide, and bismuth oxide glasses.

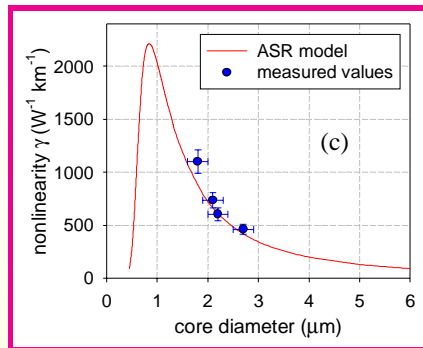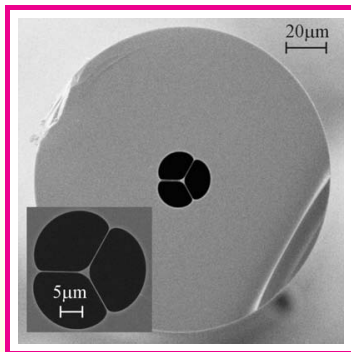- Refractive index n and n_2 follow a linear relationship.

Bismuth-Oxide Fibers

Ebendorff-Heidepriem et al., Opt. Express **12**, 5082, 2004).

- By 2004, BiO_2 fibers exhibited values of $\gamma > 1000$ W^{-1}/km near 1.55 μm when their core diameter was reduced to below 2 μm.

- $\gamma = 1100$ W^{-1}/km for the fiber with a core diameter of 2.1 μm.

- Values of $\gamma > 2000$ W^{-1}/km possible with a further reduction in the core size.

Applications of HNLFs

- Highly nonlinear fibers lead to novel nonlinear effects.

- Supercontinuum generation has attracted most attention because of its applications in metrology and biomedical imaging.

- Large Raman-induced frequency shifts allow tuning of mode-locked lasers on the long-wavelength side.

- Harmonic generation can be used to shift laser wavelength toward the blue side.

- Main advantage of using fibers as a nonlinear medium is that their nonlinear response is ultrafast.

- Instantaneous nature of the nonlinear effects can be used for high-speed switching and ultrafast signal processing.

Raman-Induced Frequency Shift (RIFS)

- The spectrum of ultrashort pulses shifts toward the red side in anomalous-dispersion regime.

- This effect was first observed in 1986; also known as the soliton self-frequency shift.

- RIFS scales with pulse width as T_0^{-4} and becomes quite large for short pulses.

- It can also occur in the normal-dispersion regime but its magnitude is relatively small: Santhanam and Agrawal, Opt. Commun. **222**, 413 (2003).

- Very large RIFS can occur in highly nonlinear fibers if pulse energy is large enough to excite a high-order soliton.

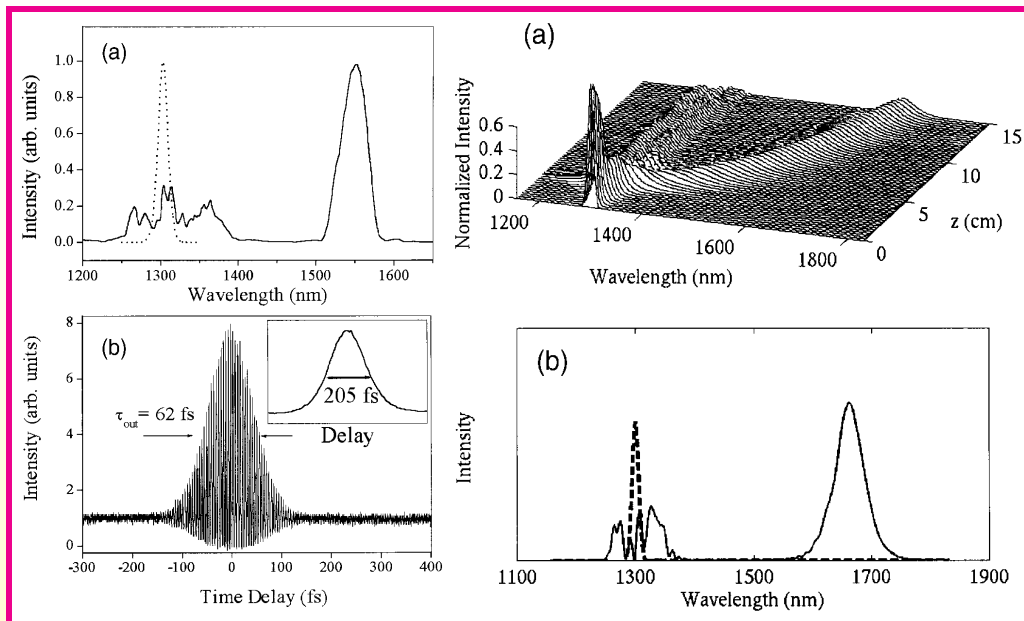- RIFS can be used for tuning wavelength of a mode-locked laser.

Experimental Evidence of RIFS

(Liu et al, Opt. Lett. **26**, 358, 2001)

Left: Measured (a) pulse spectrum and (b) autocorrelation trace.
Right: Numerical (a) spectral evolution and (b) output spectrum.

Experimental Details

- 200-fs pulses at 1.3 μm were used from a parametric oscillator pumped by a Ti:sapphire-laser.

- Pulses launched into a 15-cm-long microstructured fiber (core diameter 2–3 μm).

- Most of the pulse energy appeared in a red-shifted soliton that was considerably narrower than the input pulse (62 fs).

- RIFS of up to 350 nm (50 THz) observed experimentally.

- RIFS could be tuned as it depends on pulse's peak power.

- Numerical simulations predict the observed behavior well.

- Physical Mechanism behind large RIFS: **soliton Fission**.

Fission of High-Order Solitons

- For a pulse of with T_0 and peak power P_0, the order of a soliton is: $N = (\gamma P_0 T_0^2 / |\beta_2|)^{1/2}$.

- Third-order dispersion breaks a Nth-order soliton into N much narrower fundamental solitons of different widths.

$$T_k = \frac{T_0}{2N+1-2k}, \qquad P_k = \frac{(2N+1-2k)^2}{N^2} P_0.$$

- Spectrum of narrowest soliton shifts the most: $\Delta v_R = -\frac{4T_R |\beta_2| z}{15\pi T_1^4}$.

- When $N = 3$, the shortest soliton after fission has a width $T_0/5$.

- RIFS is enhanced for this soliton by a factor of 5^4 or 625.

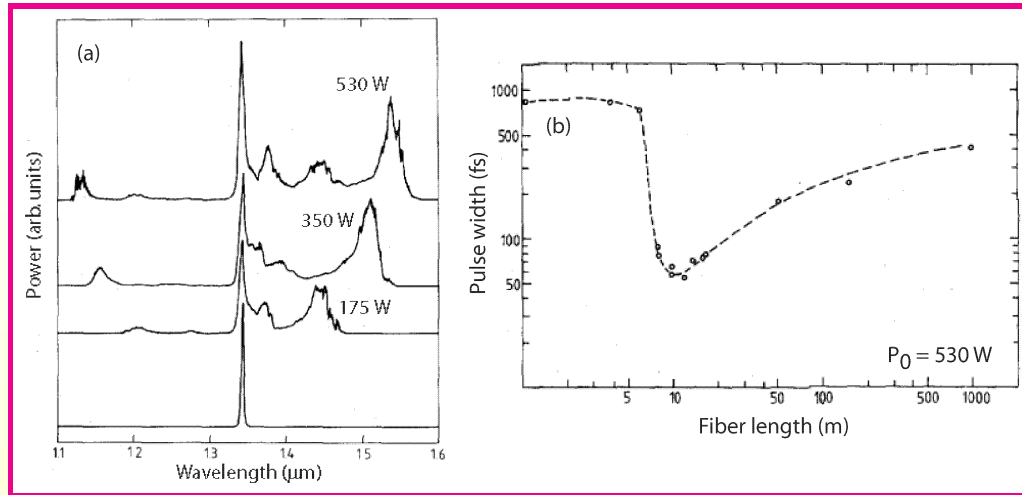- The predicted behavior agrees with the experimental data.

Experimental Evidence of Fission

(Beaud et al, IEEE JQE **23**, 1938, 1987)

- Soliton fission occurs after 7 m; pulse width drops from 830 fs to 50 fs (right).

- Different solitons undergo different red shifts (left).

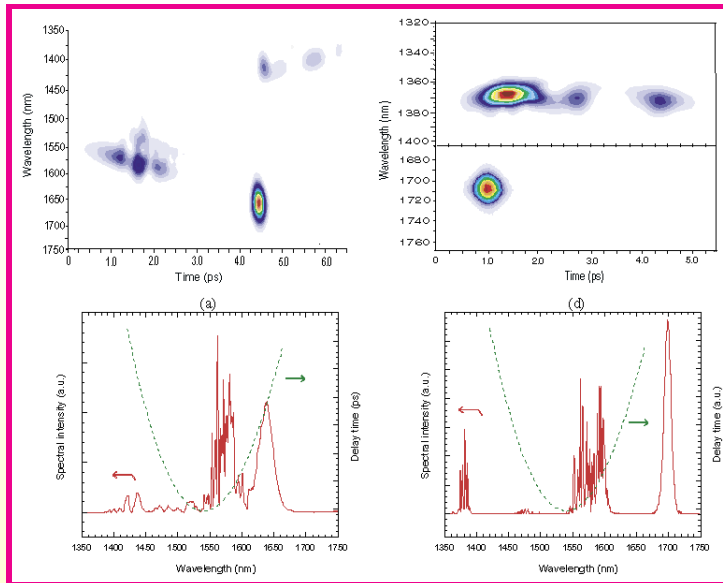- Notice a tiny peak on the blue side of the input spectrum.

X-FROG Measurements

Nishizawa and Goto, Opt. Exp. **8**, 328 (2001)

- X-FROG traces and spectra of 110-fs input pulses at the output of 10 m and 180 m long fibers.

- Note again the appearance of radiation near 1400 nm (blue side).

Resonant Dispersive Waves

- Ultrashort solitons perturbed by third-order dispersion emit dispersive waves (an example of Cherenkov radiation).

- Energy is transferred at a wavelength for which phase velocity of radiation matches that of the soliton:

$$\sum_{m=2}^{\infty} \frac{\beta_m(\omega_s)}{m!} \Omega_d^m = \tfrac{1}{2} \gamma P_s \quad (\Omega_d = \omega_d - \omega_s).$$

- Solution when dispersion up to third-order is included:

$$\Omega_d \approx -\frac{3\beta_2}{\beta_3} + \frac{\gamma P_s \beta_3}{3\beta_2^2}.$$

- Frequency shift $\Omega_d > 0$ when $\beta_2 < 0$ and $\beta_3 > 0$ (blue shift).

- Such dispersive waves propagate in the normal-GVD regime (Akhmediev et al., Phys. Rev. A **51**, 2602, 1995).
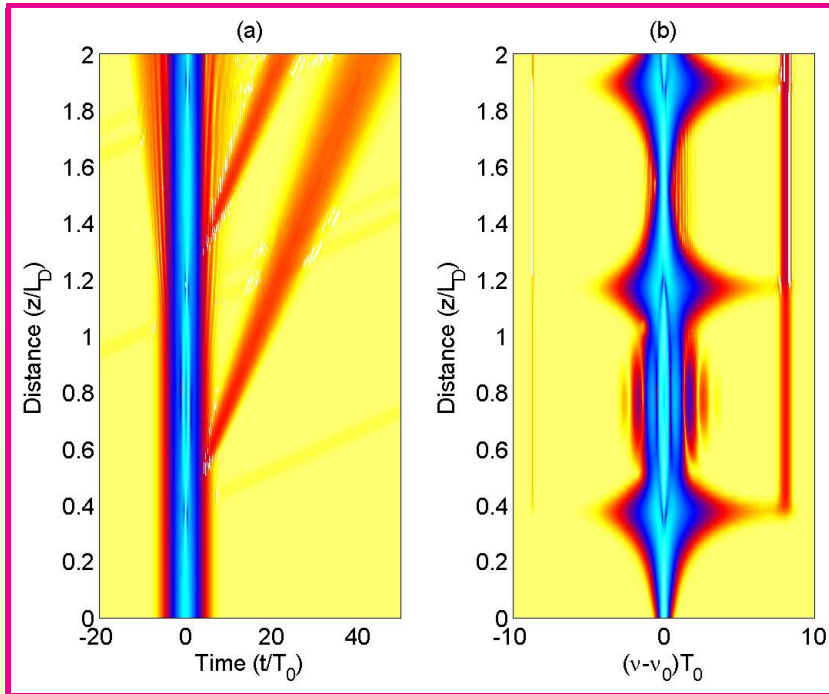
Numerical Example

- $N = 3$ soliton over $2L_D$; RIFS ignored to emphasize TOD effects.

- Dispersive wave (red vertical line) spreads in time domain.

Supercontinuum Generation

- Ultrashort pulses are affected by a multitude of nonlinear effects, such as SPM, XPM, FWM, and SRS, together with dispersion.

- All of these nonlinear processes are capable of generating new frequencies outside the input pulse spectrum.

- For sufficiently intense pulses, the pulse spectrum can becomeso broad that it extends over a frequency range exceeding 100 THz.

- Such extreme spectral broadening is referred to as **supercontinuum generation**.

- First observed in solid and gases 40 years ago; studied extensively in HNLFS after 2000.

- Recent book *Supercontinuum Generation in Optical Fibers* (Dudley and Taylor, CUP, 2010) covers it in detail.
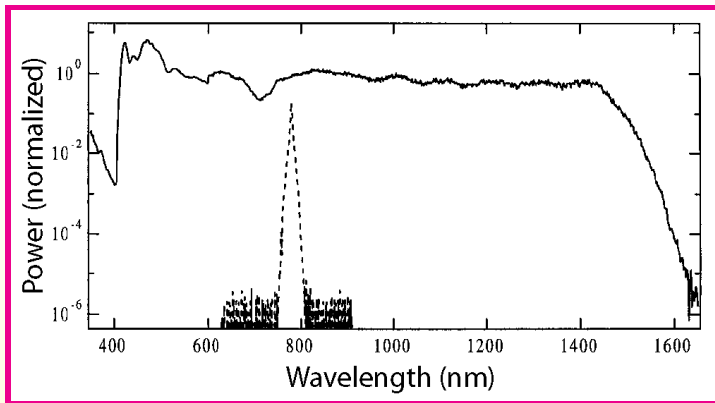
SC Generation in a Microstructured Fiber

(Ranka et al., Opt. Lett. **25**, 25, 2000)

- Output spectrum generated in a 75-cm section of microstructured fiber using 100-fs pules with 0.8 pJ energy.

- Even for such a short fiber, supercontinuum extends from 400 to 1600 nm.

- Supercontinuum is also relatively flat over the entire bandwidth.

Role of Soliton Fission

- Input pulses correspond to a higher-order soliton of large order; typically $N = (\gamma P_0 T_0^2/|\beta_2|)^{1/2}$ exceeds 10.

- Higher-order effects leads to their fission into much narrower fundamental solitons: $T_k = T_0/(2N + 1 - 2k)$

- Each of these solitons is affected by intrapulse Raman scattering.

- Spectrum of each soliton is shifted toward longer and longer wavelengths with propagation inside the fiber.

- At the same time, each soliton emits dispersive waves at different wavelengths on the blue side.

- XPM and FWM generate additional bandwidth and produce a broad supercontinuum.

Numerical Modeling of Supercontinuum

- Soliton fission studied by solving the generalized NLS equation:

$$\frac{\partial A}{\partial z} + \frac{\alpha}{2}A + i\sum_{m=2}^{M}\frac{i^m\beta_m}{m!}\frac{\partial^m A}{\partial t^m}$$
$$= i\gamma\left(1+\frac{i}{\omega_0}\frac{\partial}{\partial t}\right)\left(A(z,t)\int_0^\infty R(t')|A(z,t-t')|^2 dt'\right).$$

- It is important to include the dispersive effects and intrapulse Raman scattering as accurately as possible.

- Terms up to $M = 15$ are included in numerical simulations.

- Raman response included through the measured gain spectrum.

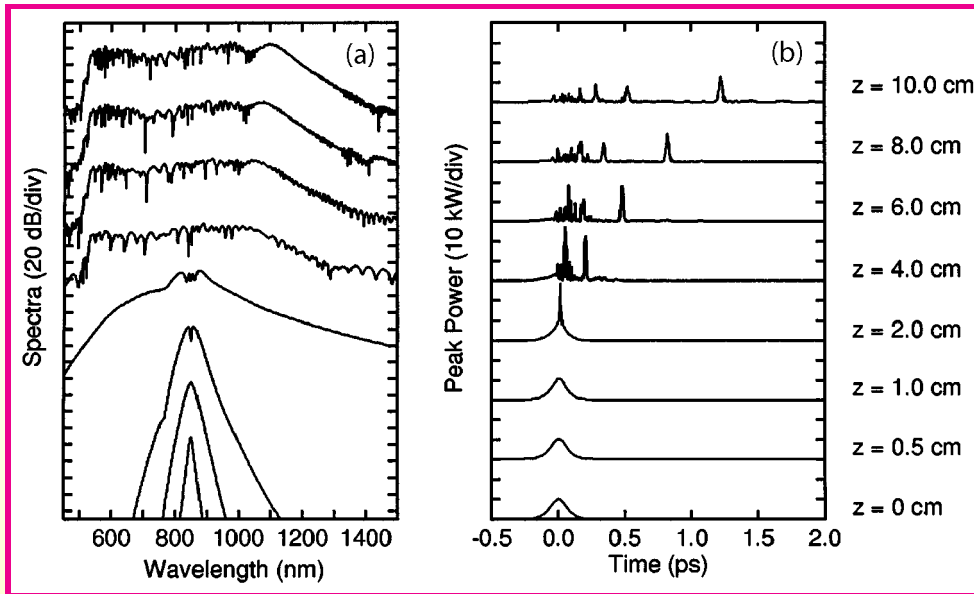- Most features observed experimentally can be understood, at least qualitatively, by such a theory.

Numerical Simulations

(a) Spectra (20 dB/div) vs Wavelength (nm): 600, 800, 1000, 1200, 1400

(b) Peak Power (10 kW/div) vs Time (ps): -0.5, 0.0, 0.5, 1.0, 1.5, 2.0 — z = 0 cm, z = 0.5 cm, z = 1.0 cm, z = 2.0 cm, z = 4.0 cm, z = 6.0 cm, z = 8.0 cm, z = 10.0 cm
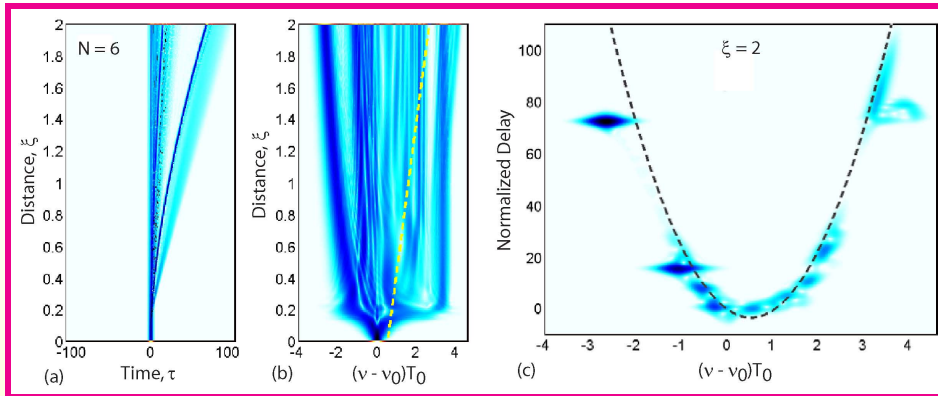
(Dudley and Coen, JSTQE **8**, 651, 2002)

- 150-fs pulses with 10-kW peak power launched into a 10-cm tapered fiber with 2.5-μm waist.

- Evolution of pulse spectrum and shape along the fiber.

Numerical Simulations (cont.)

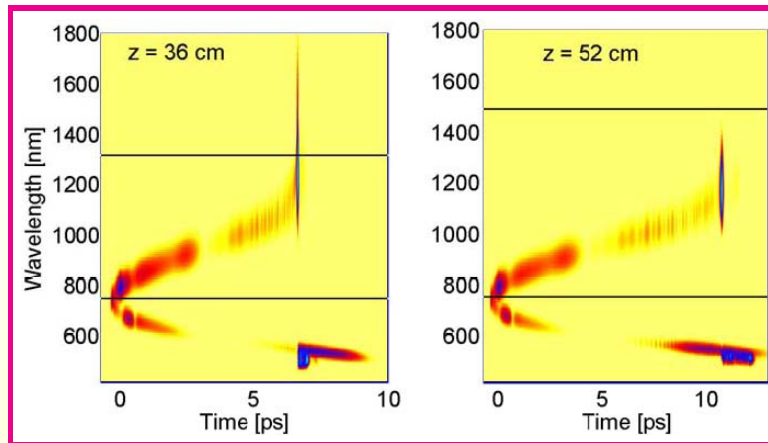(a) Time, τ (b) $(\nu - \nu_0)T_0$ (c) $(\nu - \nu_0)T_0$

- Temporal and spectral evolution of a $N = 6$ soliton over $2L_D$.

- Corresponding spectrogram at $z = 2L_D$. Dashed curve shows changes in $d\beta/d\omega$ with frequency.

- Spectrogram shows multiple solitons and their dispersive waves.

- Temporal overlap between the two leads to new effects through XPM and FWM.
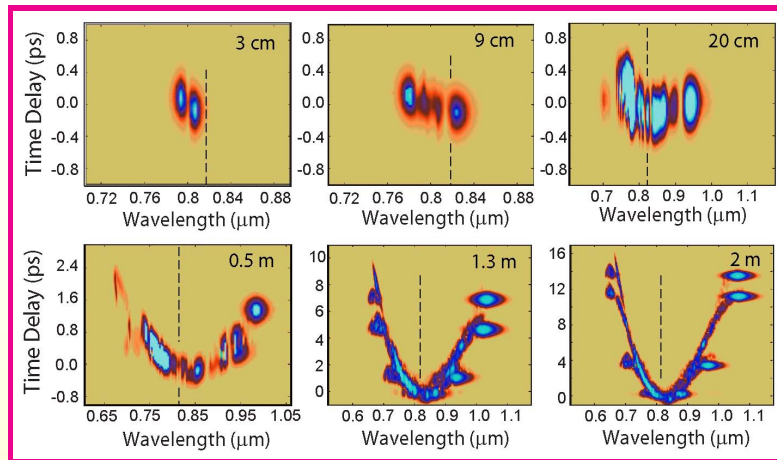
XPM-Induced Soliton Trapping

Frosz et al., Opt. Exp. **13**, 4614 (2005)

- XPM coupling can lead led to soliton-pair formation.

- Horizontal lines indicate ZDWLs of the fiber.

- Two PCFs are identical with the only difference that spacing of 1-μm-diameter air holes changes from (a) 1.2 to (b) 1.3 μm.

Evidence of Four-Wave Mixing

Gorbach et al., Opt. Exp. **14**, 9854 (2006)

- Numerical spectrograms at six locations within the fiber.

- Entire spectrum still lies in the normal-GVD regime at 3 cm.

- A Raman soliton and its dispersive wave are seen at $z = 20$ cm.

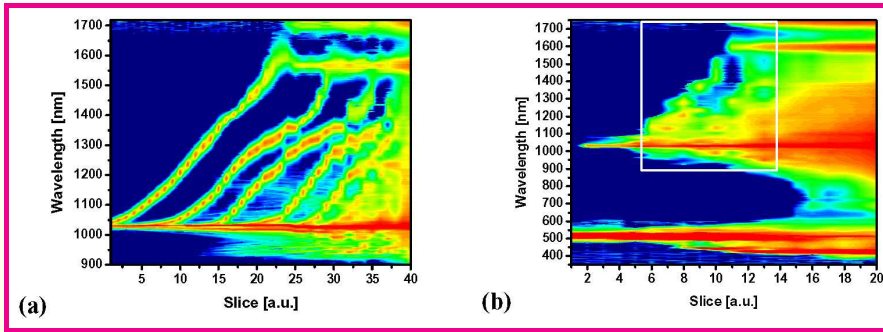- At $z = 50$ cm, we see evidence of a FWM band near 650 nm.

Pump-Probe Configuration

Schreiber et al., Opt. Exp. **13**, 9556 (2005)

- Measured spectra at the output of a 5-m-long fiber when 30-fs input pulses were propagated (a) without and (b) with weak SHG pulses.

- Fiber had two ZDWLs located at 770 and 1600 nm.

- Supercontinuum does not extends in the spectral region below 900 nm when only pump pulses are launched.

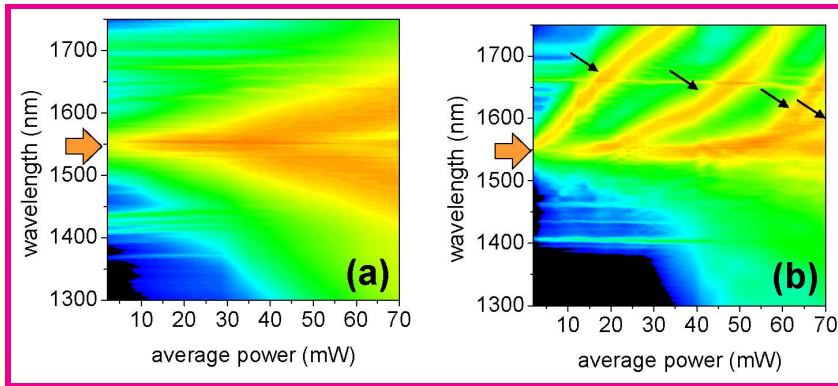- XPM effects extend the supercontinuum in the visible region.

Lead-Silicate Fibers

Omenetto et al., Opt. Exp. **14**, 4928 (2006)

- Spectra for (a) 0.57 cm and (b) 70 cm long lead-silicate PCF.

- Number of solitons with RIFS increases with P_{av} for long fiber.

- Soliton fission does not occur for the short fiber; broad supercontinuum (350 to 3000 nm) generated predominantly through SPM.

- n_2 larger by a factor of >10 for lead silicate glasses.

Lead-Silicate Fibers (cont.)
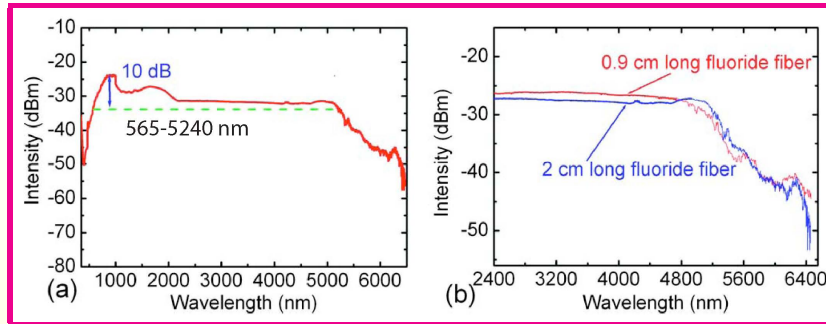
Qin et al., Appl. Phys. Lett. **95**, 161103 (2009)

- Largest SC bandwidth realized in 2009 by pumping a 2-cm fluoride fiber with 180-fs pulses power at 1450 nm.

- (a) Output spectrum at 20-mW average power ($P_0 \sim 50$ MW).

- (b) Virtually the same bandwidth is obtained for the shorter fiber.

- Soliton fission does not occur for such short fibers; broad supercontinuum generated predominantly through SPM.
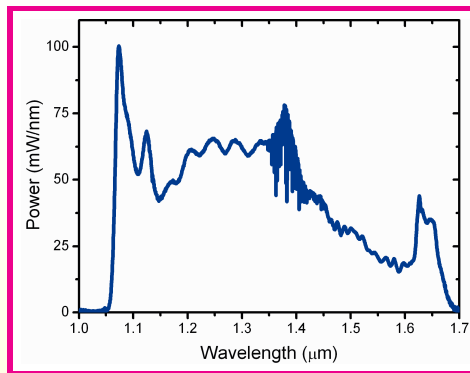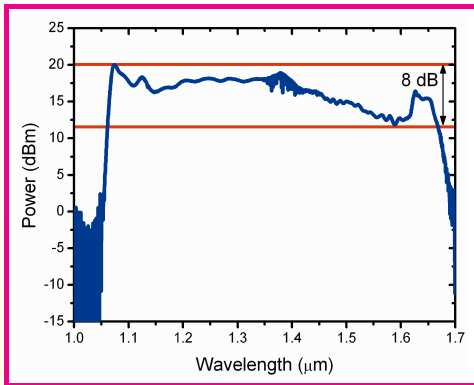
Continuous-Wave Supercontinuum

Cumberland et al., Opt. Exp. **116**, 5954 (2008)

- Supercontinuum on (a) semi-log and (b) linear scales at the end of a 20-m-long PCF pumped with 44 W of CW power at 1070 nm.

- Fiber exhibited two ZDWLs near 810 and 1730 nm.

- Output power was 29 W, and spectral power density exceeded 50 mW/nm up to 1400 nm.

- Useful as a supercontinuum source for biomedical imaging.

CW Supercontinuum (cont.)
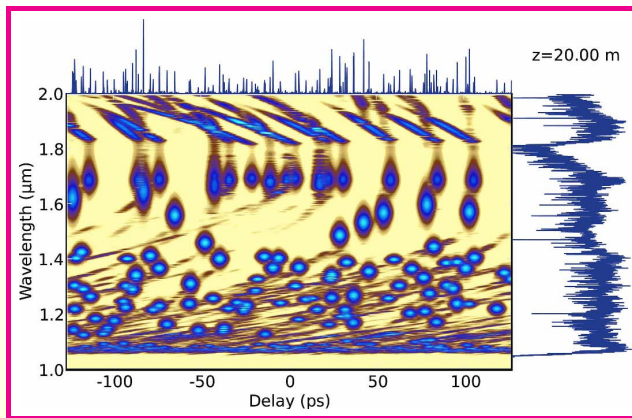
Cumberland et al., Opt. Exp. **16**, 5954 (2008)

- Formation of fundamental solitons (round objects) of different widths through modulation instability (no fission).

- Spectrum of a soliton stops shifting near 1730 nm.

- Cigar-like objects at $\lambda >$1730 nm represent dispersive waves.
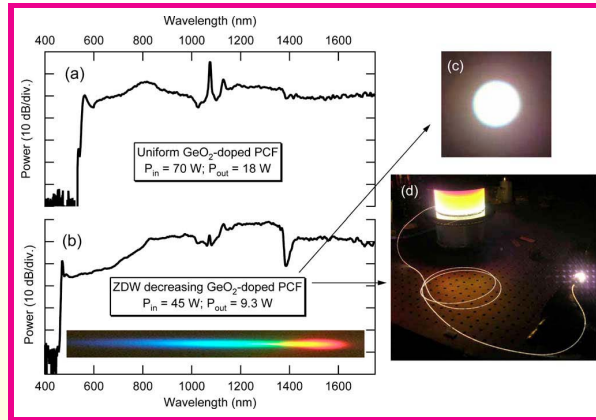
- FWM generates new spectral components near 1900 nm.
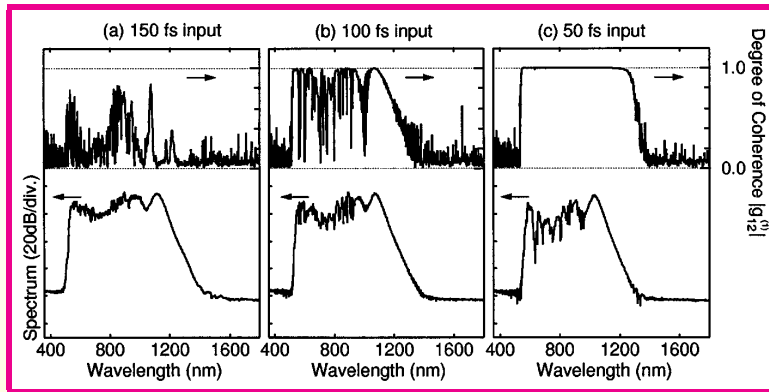
CW Supercontinuum (cont.)

Kudlinski et al., Opt. Lett. **34**, 3631 (2009)

- Visible CW Supercontinuum created by 2009 using PCFs with Ge-doped cores.

- Only 45 W of CW power needed for a tapered-core PCF.

- Photographs of output dispersed by a prism, (c) white spot, and (d) fiber spool are also shown.

Coherence Properties

Dudley and Coen, JSTQE **8**, 651 (2002)

- Degree of spectral coherence: $g_{12}(\omega) = \dfrac{\langle \tilde{A}_1^*(L,\omega)\tilde{A}_2(L,\omega)\rangle}{[\langle|\tilde{A}_1(L,\omega)|^2\rangle\langle|\tilde{A}_2(L,\omega)|^2\rangle]^{1/2}}$

- It is measured by interfering two successive pulses in a pulse train and recording the contrast of spectral fringes.

- Shorter pulses provide a more coherent supercontinuum.

Optical Rouge Waves

- Pulse-to-pulse fluctuations degrade the coherence of a supercontinuum.

- They give rise to an optical analog of oceanic rogue waves (rare but giant water waves) that can form in oceans.

- Such waves are characterized by their 'L-shaped' statistics.

- Optical analog of rogue waves first observed in 2007 by Solli et al in the context of supercontinuum generation.

- Recent work has clarified their origin and also shows how they can be controlled.

- Optical rogue waves may be connected to Akhmediev breathers and the Peregrine soliton found in the context of the NLS equation.
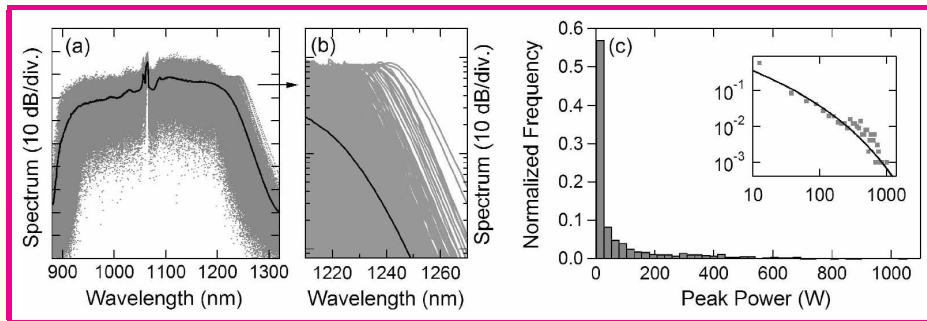
Optical Rouge Waves (cont.)

Dudley et al., Opt. Express **16**, 3644 (2008)

- Generalized NLS equation can produce the L-shaped statistics of optical rogue waves if it is solved for multiple noisy input pulses.

- Noisy 5-ps Gaussian pulses propagated inside a 20-m-long PCF.

- Spectral power fluctuates by $>$20 dB even when only quantum noise is included (one photon per frequency bin).

- Peak power of shortest soliton exhibits **L-shaped statistics**.
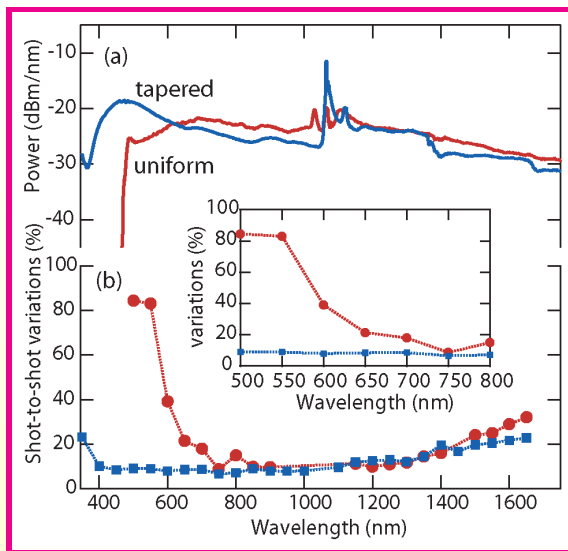
Control of Rouge Waves
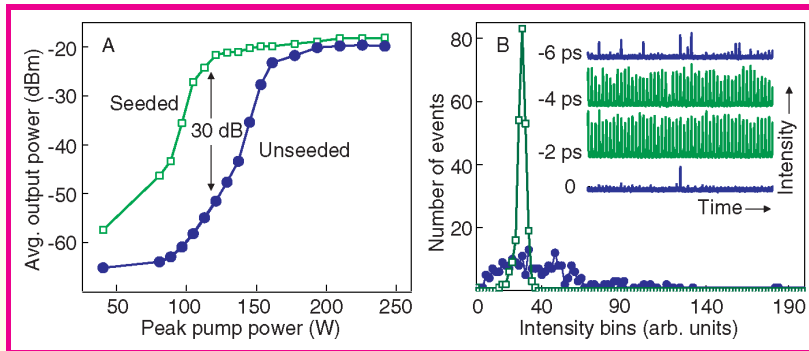
Solli et al., Phys. Rev. Lett. **101**, 233902 (2008)

- SC initiated by modulation instability (MI) exhibited Rogue-wave features (4-ps pulses at 1550 nm).

- Rogue-wave statistics changed when MI was initiated by launching seed pulses at 1630 nm.

- Relative delay between the pump and seed pulses played an important role.

Control of Rouge Waves (cont.)

Kudlinski et al., Opt. Express **18**, 274452 (2010)

- Rogue-wave statistics controlled by tapering a PCF.

- Tapering changes dispersive properties along fiber length.

- Shot-to-shot variations decreased from >80% to below 20%.

Periodic Solutions of the NLS Equation

- Optical rouge waves also appear in the context of Raman amplification and FWM.

- Is there is an underlying common origin of rogue waves?

- Any nonlinear mechanism that exhibits optical gain and can transfer power from a pump to noise may give rise to optical rouge waves.

- In some cases, optical rouge waves may be related to the periodic and algebraic solutions of the NLS equation.

$$A(z,T) = \sqrt{P_0}\, e^{i\xi} \left[\frac{(1-4a)\cosh(b\xi) + ib\sinh(b\xi) + \sqrt{2a}\cos(\Omega T)}{\sqrt{2a}\cos(\Omega T) - \cosh(b\xi)} \right]$$

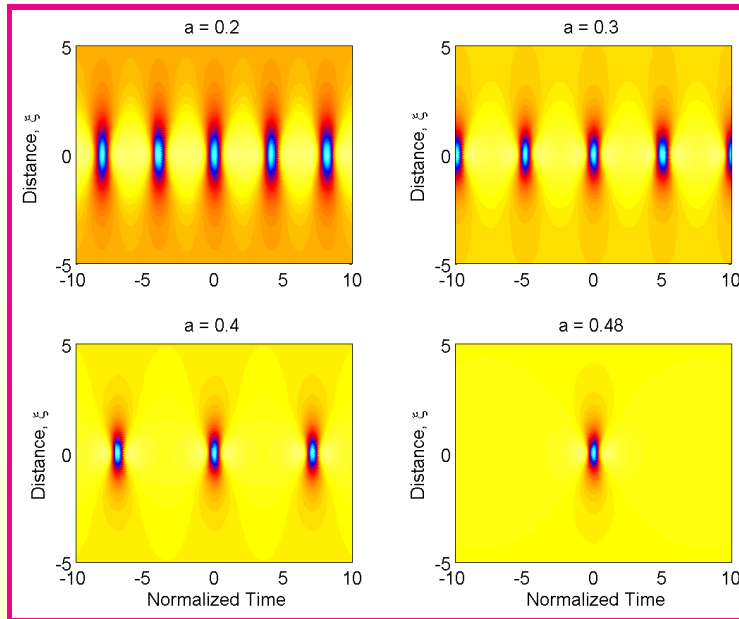$a = \frac{1}{2}[1 - (\Omega/\Omega_c)^2]$, $b = \sqrt{8a(1-2a)}$, $\Omega_c = \sqrt{4\gamma P_0/\beta_2}$, $\xi = z/L_D$.

N. Akhmediev and V. I. Korneev, *Theor. Math. Phys.* **69**, 1089 (1986).

Akhmediev breather

- Periodic solutions of NLS equation are called Akhmediev breathers.

- Parameter $a = \frac{1}{2}[1 - (\Omega/\Omega_c)^2]$ controls the period $(\Omega_c = \sqrt{4\gamma P_0/\beta_2})$.

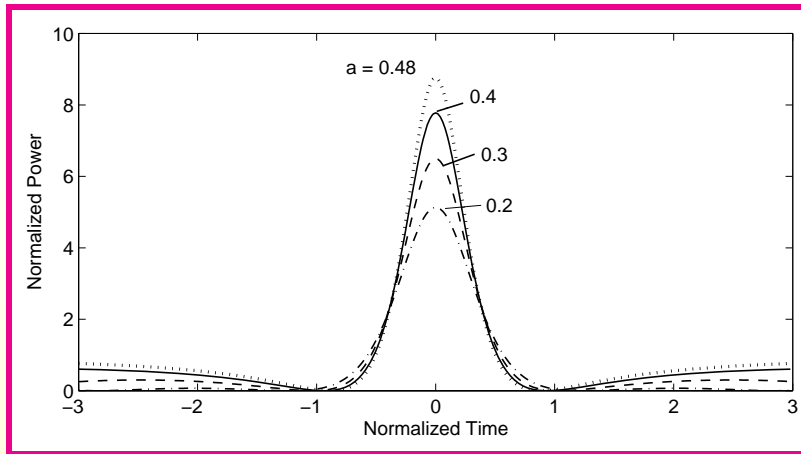- Period becomes infinite as $a \to \frac{1}{2}$ (Peregrine soliton).

Peregrine soliton

- In the limit $a \to \frac{1}{2}$, pulse shape corresponds to the Peregrine soliton:

$$A(z,T) = \sqrt{P_0}\, e^{i\xi} \left[1 - \frac{4(1+2i\xi)}{1+(\Omega_c T)^2 + 4\xi^2} \right] \quad (\xi = z/L_D).$$

- This algebraic solution has the largest amplitude and may be behind the formation of optical rogue waves.

Observation of Peregrine soliton

- Peregrine soliton observed in a 2011 experiment using MI inside a 8.4-km-long fiber (SMF-28).

- Input in the form of a modulated CW beam ($P_0 = 0.8$ W).

- Amplitude modulated at 16 GHz with 30% contrast.

- Results (left) in agreement with theory (right).

- Temporal evolution (top); spectral evolution (middle); Shape and spectrum (bottom).
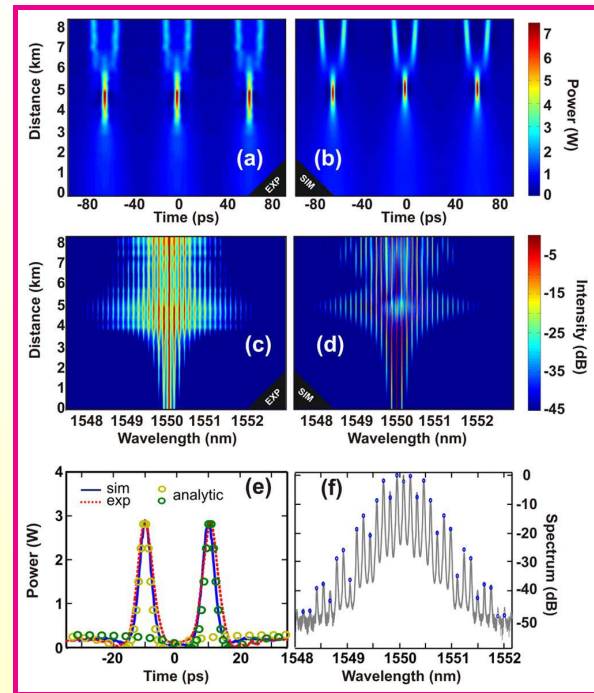
Hammani et al., Opt. Lett. **36**, 112 (2011)

Conclusions

- Recent advances in designing HNLFs have led to a number of novel applications of nonlinear fiber optics.

- Raman-induced frequency shift can be used to tune ultrashort pulses on the longer-wavelength side.

- Supercontinuum research led to fundamental understanding of concepts such as soliton fission, RIFS suppression, and optical rogue waves.

- Supercontinuum generated in HNLFs is useful for metrology, biomedical imaging, and other applications requiring wideband sources.

- Photonic bandgap fibers whose core is filled with nonlinear gases and liquids are likely to lead to many other advances.

- This is an exciting are of research for new graduate students.

Further Reading

- R. R. Alfano, Ed., *The Supercontinuum Laser Source*, 2nd ed. (Springer, New York, 2006).

- J. M. Dudley et al., "Supercontinuum generation in photonic crystal fibers," *Rev. Modern Phys.*, **78**, 1135-1184 (2006).

- G. P. Agrawal, *Applications of Nonlinear Fiber Optics*, 2nd ed. (Academic Press, 2008).

- J. M. Dudley and J. R. Taylor, *Supercontinuum Generation in Optical Fibers* (Cambridge University Press, 2010).

- G. P. Agrawal, *Nonlinear Fiber Optics*, 5th ed. (Academic Press, 2013).